

Solid-State Nanopore Analysis on Conformation Change of p53TAD-MDM2 Fusion Protein Induced by Protein-Protein Interaction

Hongsik Chae,^{1,‡} Dong-Kyu Kwak,^{2,3,‡} Mi-Kyung Lee,² Seung-Wook Chi,^{2,3,} and Ki-Bum Kim^{1,‡,*}*

¹Department of Materials Science and Engineering, Seoul National University, Seoul 08826, Korea

²Disease Target Structure Research Center, KRIBB, Daejeon 34141, Korea

³Department of Proteome Structural Biology, KRIBB School of Bioscience, Korea University of Science and Technology, Daejeon 34113, Korea

[†]Research Institute of Advanced Materials (RIAM), Seoul National University, Seoul 08826, Korea

Author Contributions

[‡]These authors contributed equally to this work

Corresponding Authors:

Ki-Bum Kim: kibum@snu.ac.kr

Seung-Wook Chi: swchi@kribb.re.kr

1. Nanopore device fabrication processes

100 nm-thick freestanding LPCVD SiN_x membrane on Si substrate was prepared by photolithography and KOH wet chemical etching. Separately, LPCVD a-Si (200 nm) was deposited on quartz substrate and patterned on top (2 μm) and bottom side (300 μm) using photolithography for HF wet etching of quartz.¹ The freestanding SiN_x membrane was transferred on top side of a-Si layer of the quartz substrate as illustrated in Figure S1. The SiN_x membrane and quartz substrate was placed on the hot plate (~90°C). After 3 hours, Si support was removed and the transferred SiN_x layer was remained. Next, the SiN_x membrane was reduced to a desirable thickness using reactive ion etching. Using CF₄ gas (50 sccm) under base pressure of 0.05 Torr and 50 W RF power was used to etch the SiN_x membrane. Then, the quartz chip was annealed in 400°C for 4 hours. Finally, the quartz chip was placed in the custom-made TEM holder for drilling nanopore in the SiN_x membrane using highly focused electron beam. Oxygen plasma was treated on both side of nanopore chip for 2 minutes (15 mA, 0.20 mbar) for induce hydrophilicity to the surface. After that, nanopore chip was assembled using custom-made Teflon flow cell with PDMS gasket for stable measurement.

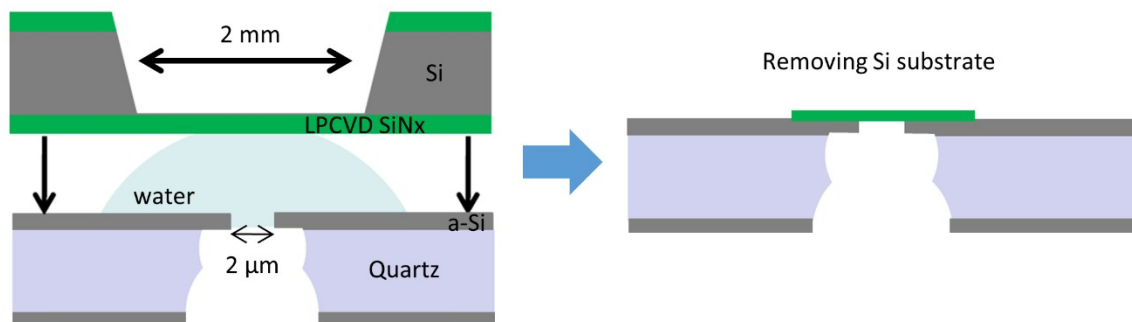


Figure S1. Schematic illustration of LPCVD SiN_x transfer on quartz substrate (not to scale).

2. Current drop histogram of the translocation events

For further analysis of nutlin-3 effect on nanopore signal, current drop histogram for free, 1:1, 1:5, and 1:10 are analyzed (Figure S2). In the sample without nutlin-3, we obtained two distinct population in the fractional current ($\Delta I/I_0$) histogram for type I signal. The mean fractional current ($\langle \Delta I/I_0 \rangle$) was extracted by fitting the Gaussian function as $\langle \Delta I/I_0 \rangle \sim 0.036$ and ~ 0.070 , respectively. The first population in the histogram accounts for bumping event, while the second population is regarded as single molecule translocation of MLP. Since current drop less than $\Delta I/I_0 < 0.035$ exhibits dwell time of $\sim 5\mu\text{s}$ in the scatter plot (Fig 4, see text), we regarded those event as bumping event. After the addition of equimolar nutlin-3, two population was also appeared with similar fractional current drop to free, showing $\langle \Delta I/I_0 \rangle \sim 0.034$ and ~ 0.071 , respectively. The further increase of nutlin-3 concentration on the MLP to 5 and 10-fold molar ratio of nutlin-3 into the MLP shows $\langle \Delta I/I_0 \rangle \sim 0.077$ and 0.068 for 1:5 and 1:10, respectively. The similar value of $\langle \Delta I/I_0 \rangle$ implies that nutlin-3 does not change a net volume of protein but identical event for type I event in all concentration of nutlin-3.

Obviously, no bumping event was detected in type II event for all nutlin-3 concentration. As we designed, we found two intra-peaks in the type II event. As we designed, the intra-peaks reflect the volume of GST-p53TAD and MDM2. Because the volume of GST-p53TAD is larger than that of MDM2, a larger peak is considered to the transient blockage of GST-p53TAD in the nanopore. Figure S2 e-g shows the fractional current histogram of GST-p53 peak in the type II. On the other hand, the most of MLP volume is occupied GST-p53TAD, the mean fractional current of type II ($\langle \Delta I/I_0 \rangle \sim 0.073$) is reflected similar value to the type I event.

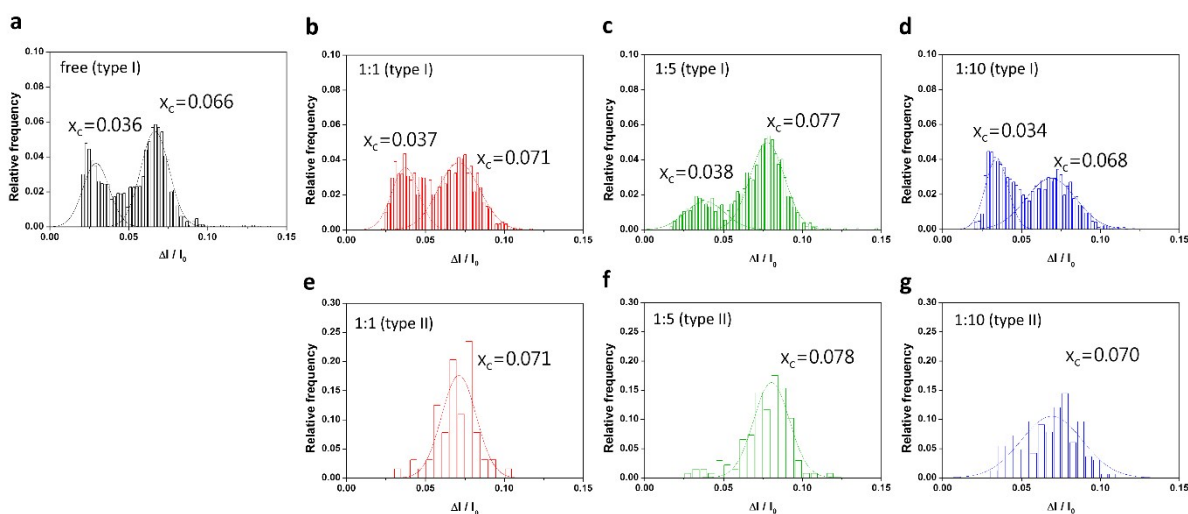


Figure S2. Histogram of fractional current. The current drop histogram of type I event after addition of nutlin-3 in molar ratio of free (a), 1:1 (b), 1:5 (c), and 1:10 (d), showing no significant change. The histogram of type II event for 1:1 (e), 1:5 (f), and 1:10 (g). All histogram was fitted by the Gaussian functions with the center of the peak (X_c).

3. Dwell time histogram of intra-peak of type II events

We additionally analyzed dwell time of type II event intra-peaks, which represents traversing time for GST-p53TAD, MDM2, and amino acid linker. Dwell time of type II intra-peak was defined as t_H , t_M , and t_L as shown in figure S3a inset. Dwell time histogram for t_H was fitted by the Gaussian function with mean value, $\langle t_H \rangle$, as 6.09 ± 2.69 , 5.85 ± 5.44 , and 5.70 ± 3.18 μ s for 1:1, 1:5, and 1:10, respectively. For $\langle t_M \rangle$, we obtained lower value of 4.62 ± 2.94 , 5.40 ± 4.91 , and 4.59 ± 3.09 μ s for 1:1, 1:5, and 1:10, respectively. Data for t_L , which structurally reflects amino acid linker in our designed complex, exhibited short dwell time that fitting the Gaussian function to the data was not appropriated. We used the exponential decay function to evaluate the characteristic time for t_L yields 2.32, 2.44, and 2.15 μ s for 1:1, 1:5, and 1:10, respectively.

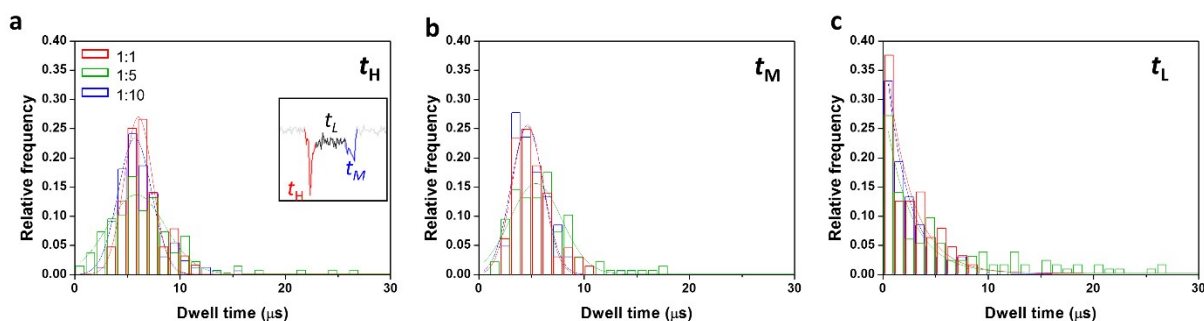


Figure S3. Histogram of dwell time for type II inter-event. Inset (a) represents the local dwell time of type II event (t_H , t_M and t_L). Dwell time histogram was fitted by the Gaussian function for t_H (a) and t_M (b), while dwell time histogram for t_L was fitted exponential decay function with characteristic time of 2.32, 2.44, and 2.15 μs for 1:1, 1:5, and 1:10, respectively.

4. Continuous current trace for protein translocation

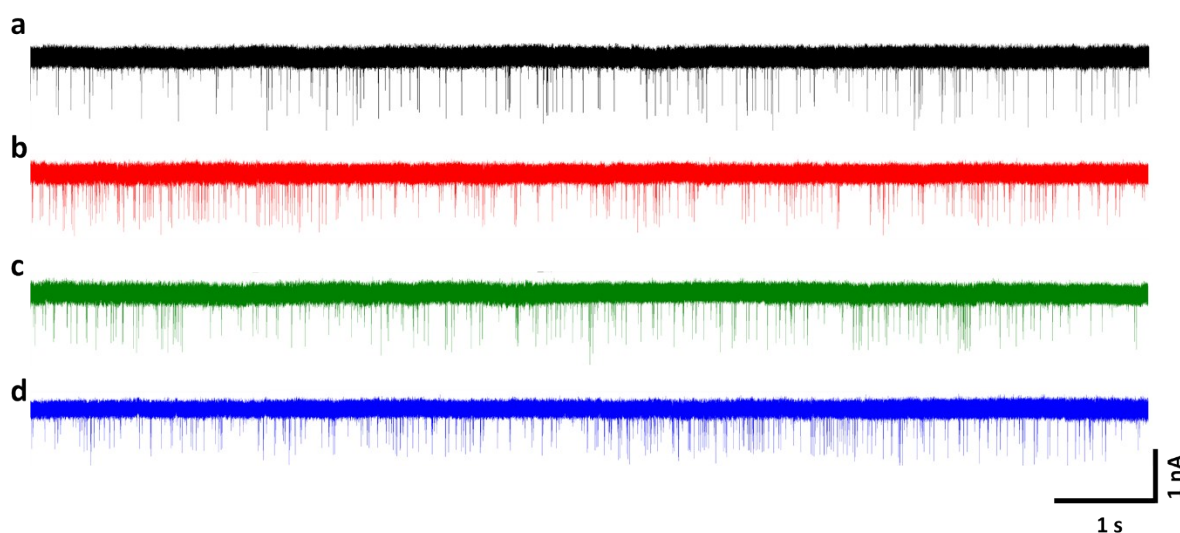


Figure S4. Continuous current-time trace for (a) free, (b) 1:1, (c) 1:5, and (d) 1:10. Data were acquired 4.16 MHz sampling rate and low-pass filtered at 500 kHz.

5. Power spectrum density of the nanopore signal

To investigate the noise characteristics of the nanopore, the power spectrum density (PSD) of the nanopore signal measured at 0 mV and 200 mV are presented in Figure S5. The noise PSD was fitted to the polynomial form of $S = Af^\beta + B + Cf + Df^2$, where f is frequency in Hz and β is the fitting parameter ($0 < \beta < 2$). The parameters A , B , C , and D represent Flicker, Johnson (Nyquist), dielectric, and amplifier noise, respectively.² The corresponding fitting parameters are tabulated in Table S1.

Table 1. Noise parameters of the nanopore device under 100 mV and 200 mV.

Noise parameters	0 mV	200 mV
<i>A</i>	1.77×10^{-2}	4.95
<i>B</i>	1.58×10^{-3}	5.89×10^{-3}
<i>C</i>	1.39×10^{-8}	5.19×10^{-9}
<i>D</i>	0	0
β	1	1
<i>I</i> _{rms} (pA)	38.76	51.76

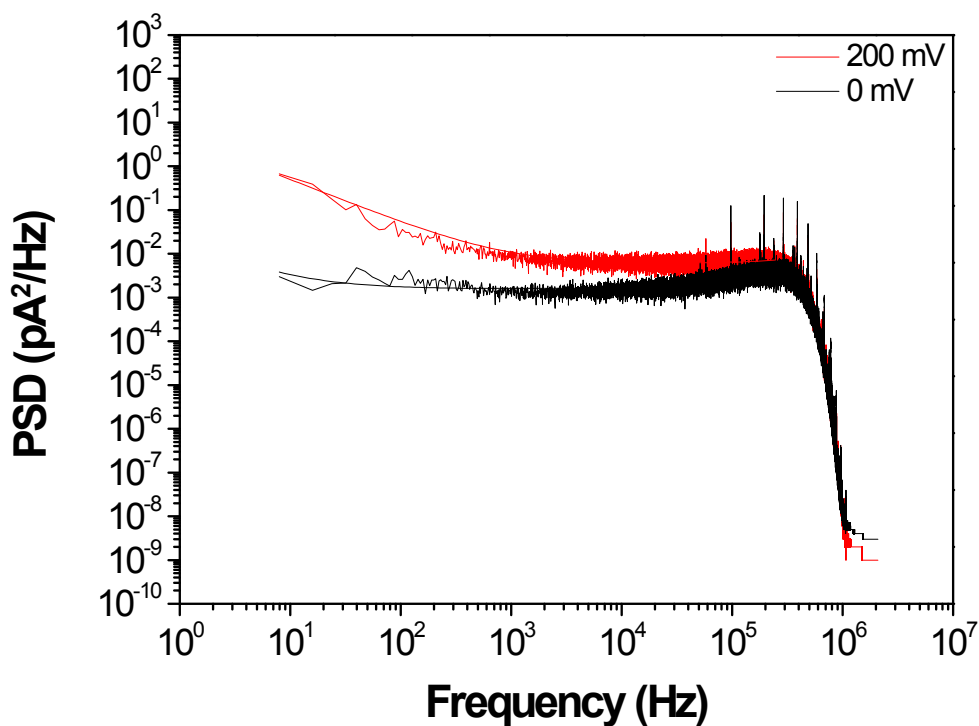


Figure S5. Power spectrum of silicon nitride nanopore signal with 1M KCl in 1 × PBS solution under 200 mV electric potential. Data was acquired using 4.16 MHz sampling rate and low-pass filtered at 500 kHz.

REFERENCES

1. M.-H. Lee, A. Kumar, K.-B. Park, S.-Y. Cho, H.-M. Kim, M.-C. Lim, Y.-R. Kim and K.-B. Kim, *Scientific reports*, 2014, **4**, 7448.
2. V. Dimitrov, U. Mirsaidov, D. Wang, T. Sorsch, W. Mansfield, J. Miner, F. Klemens, R. Cirelli, S. Yemenicioglu and G. Timp, *Nanotechnology*, 2010, **21**, 065502.